

Supplemental Data for:
Dixon et al., Structure 12, pp. 2161-2171

Unscaled Gō Model Simulations on the FAT Domain

DMD simulations of the FAT domain folding transition were initially performed using the unscaled Gō model, where all native contacts are assigned the same pair-wise potential energy. An intermediate state was detected in the unscaled DMD simulations corresponding to the folding trajectory of the FAT domain. A typical snapshot of the intermediate state ensemble near the middle of the unfolding transition indicates that helix 1 separates from the helix bundle and loses helical structure in the initial stages of protein unfolding. It has been pointed out (Dokholyan et al., 2003) that protein structures possess a posteriori information about interactions within the protein that determine protein-folding properties. This relationship between protein topology and folding dynamics has been proven in a number of protein-folding studies (Clementi et al., 2000; Shakhnovich, 1997). Not surprisingly, based on simple topological considerations (unscaled Gō model), we observe that the FAT domain samples an intermediate conformation that is consistent with emerging data relating conformational dynamics to FAK function. However, even around the midpoint of the transition this intermediate state is weakly populated during the simulation time (approximately 10^6 collisions) for the unscaled simulations.

Supplemental Experimental Procedure 1

Chemical Denaturation of the FAT Domain Using Guanidine Hydrochloride

Chemical denaturation of the FAT domain was observed by monitoring the ellipticity

at 222 nm on a Applied Photophysics π^* -180 Spectrometer (Applied Photophysics Ltd., UK) with a Microlab 500 series titration apparatus (Hamilton Company, Reno, NV). Two samples were mixed to progressively increase the concentration of denaturant without changing the concentration of the protein and buffer using withdrawal/infusion pumps. The protein sample contained 3.0 μ M purified FAT domain, 250 mM potassium phosphate buffer (pH 6.0), 150 mM sodium chloride, and 0.1% sodium azide. The second sample was the same, except for the addition of 6.0 M guanidine hydrochloride. A nonlinear least-squares global fitting of the denaturation curve (Supplemental Figure S1) was performed using the method of Santoro and Bolen to determine the free energy of unfolding in the absence of denaturant (Santoro and Bolen, 1988).

Supplemental Experimental Procedure 2

Scaling the G \bar{o} Model Using Hydrogen Exchange Protection Factors

Under conditions where the folded state of a protein is highly favored, hydrogen exchange for most of the residues is governed by local fluctuations around the native structure (Bahar et al., 1998; Vendruscolo et al., 2003). In the EX2 limit, we make an approximation in the $G\bar{o}$ model that the free energy difference (in reduced units of $k_B T$) between the exchange-competent (O) and exchange-incompetent (C) states can be described in terms of the native contacts:

$$\ln P_i = - \langle \sum_j \Delta_{ij} \epsilon_{ij} \rangle_o - (- \langle \sum_j \Delta_{ij} \epsilon_{ij} \rangle_c) = \sum_j f_{ij}^C \epsilon_{ij} - \sum_j f_{ij}^O \epsilon_{ij} ,$$

where $\|\Delta_{ij}\|$ is the protein contact matrix, the elements of which are defined to be 1 if the distance between the C $^\beta$ atoms (C $^\alpha$ for Gly) of residues i and j is less than 7.5 Å,

and 0 otherwise. $f_{ij}^C = \langle \Delta_{ij} \rangle^C$ and $f_{ij}^O = \langle \Delta_{ij} \rangle^O$ are the probabilities of forming contacts between residues i and j , determined by averaging over the states in which residue i is exchange-incompetent (C) and exchange-competent (O), correspondingly. The summation is taken over all residues j that form native contacts with residue i .

We assume that protection from hydrogen exchange is effectively due to the formation of contacts in the $G\bar{O}$ model. When residue i is exchange-competent (O), the probability of forming a contact between residues i and j is low; conversely, when residue i is exchange-incompetent (C), the probability of forming a contact between residues i and j is high. Therefore,

$$f_{ij}^C \gg f_{ij}^O, \text{ and}$$

$$\ln P_i = \sum_j f_{ij}^C \varepsilon_{ij} - \sum_j f_{ij}^O \varepsilon_{ij} \approx \sum_j f_{ij}^C \varepsilon_{ij}.$$

f_{ij}^C can be decomposed as:

$$f_{ij}^C = p^{C|F} f_{ij}^{C|F} + p^{C|U} f_{ij}^{C|U},$$

where $f_{ij}^{C|F}, f_{ij}^{C|U}$ are the probabilities of forming contacts between residues i and j when residue i is exchange-incompetent (C) in the folded and unfolded states, respectively. $p^{C|F}, p^{C|U}$ are the corresponding probabilities of being in the folded and unfolded states, given that residue i is exchange-incompetent (C).

Under native conditions, $p^{C|F} \approx 1 \gg p^{C|U}$, so that $f_{ij}^C \approx p^{C|F} f_{ij}^{C|F} \approx f_{ij}^{C|F}$.

Moreover, we have $f_{ij}^{C|F} \approx f_{ij}^F$ since

$$f_{ij}^F = f_{ij}^{C|F} + f_{ij}^{O|F} \text{ and } f_{ij}^{C|F} \approx 1 \gg f_{ij}^{O|F},$$

where f_{ij}^F is the probability of forming a contact between residues i and j in the folded state ensemble. $f_{ij}^{O|F}$ is the probability of forming a contact between residues

i and j in the folded state ensemble, given that residue i is exchange-competent (O).

Thus, we are able to make the approximation:

$$\ln P_i \approx \sum_j f_{ij}^F \varepsilon_{ij} \approx \sum_j \varepsilon_{ij} ,$$

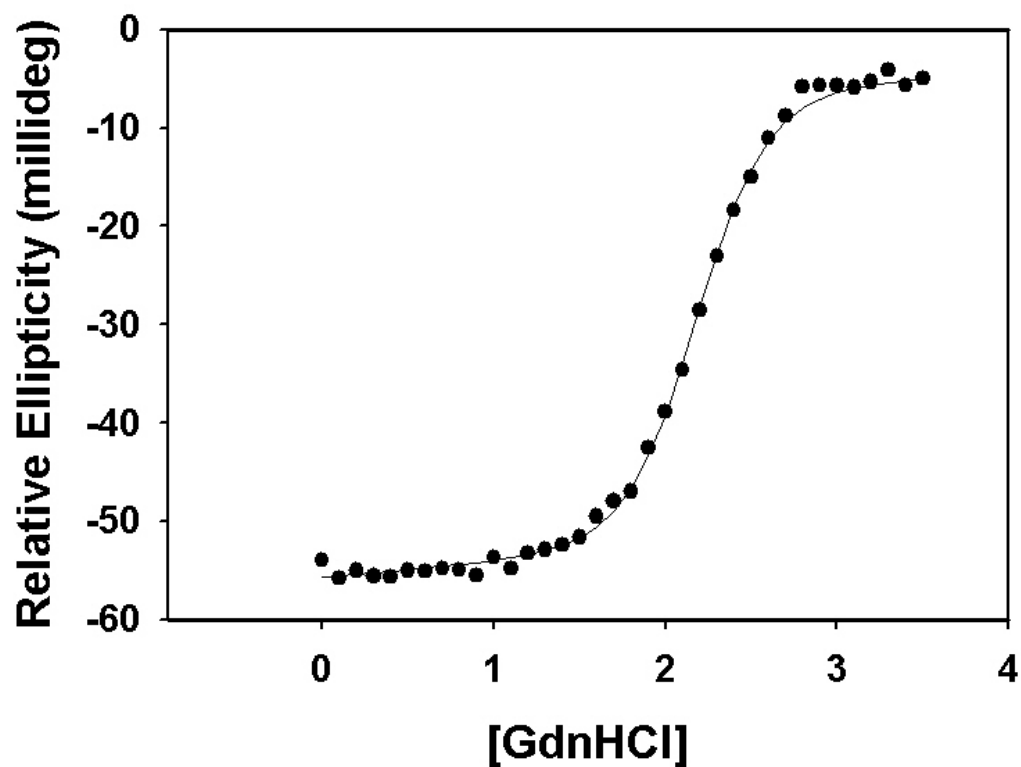
where f_{ij}^F is the probability of forming a contact between residues i and j in the folded state ensemble.

Supplemental Table S1. A Complete List of the Amide Proton Hydrogen Exchange Rates for the FAT Domain of FAK

Residue	k_{ex} (10^{-3} min^{-1})	Residue	k_{ex} (10^{-3} min^{-1})	Residue	k_{ex} (10^{-3} min^{-1})	Residue	k_{ex} (10^{-3} min^{-1})
G908	Not Assigned	P945	N/A	R982	CLEANEX	K1019	-
S909	-	A946	-	E983	-	Q1020	13 ± 6
P910	N/A	P947	N/A	I984	Not Assigned	M1021	97
G911	Not Assigned	P948	N/A	E985	9.4 ± 0.8	L1022	11 ± 1
I912	CLEANEX	E949	-	M986	Not Assigned	T1023	-
S913	CLEANEX	E950	Not Assigned	A987	4.7 ± 0.3	A1024	-
G914	CLEANEX	Y951	-	Q988	2.05 ± 0.08	A1025	Not Assigned
G915	CLEANEX	V952	-	K989	Not Assigned	H1026	15 ± 6
G916	CLEANEX	P953	N/A	L990	7.9 ± 0.6	A1027	Not Assigned
G917	CLEANEX	M954	-	L991	-	L1028	1.01 ± 0.04
G918	CLEANEX	V955	-	N992	Not Assigned	A1029	0.95 ± 0.05
I919	CLEANEX	K956	-	S993	49	V1030	Not Assigned
R920	CLEANEX	E957	-	D994	8.0 ± 0.8	D1031	0.83 ± 0.07
S921	CLEANEX	V958	Not Assigned	L995	1.71 ± 0.06	A1032	3.3 ± 0.6
N922	CLEANEX	G959	14 ± 1	A996	2.6 ± 0.2	K1033	1.22 ± 0.06
D923	CLEANEX	L960	13 ± 2	E997	1.57 ± 0.06	N1034	Not Assigned
K924	-	A961	20 ± 4	L998	0.15 ± 0.03	L1035	-
V925	-	L962	2.7 ± 0.4	I999	0.23 ± 0.03	L1036	0.20 ± 0.03
Y926	-	R963	Not Assigned	N1000	4.1 ± 0.1	D1037	14 ± 4
E927	-	T964	-	K1001	13 ± 3	V1038	1.10 ± 0.05
N928	-	L965	22 ± 3	M1002	3.6 ± 0.3	I1039	0.46 ± 0.03
V929	-	L966	12 ± 1	K1003	23 ± 7	D1040	10 ± 1
T930	-	A967	4.9 ± 0.4	L1004	22 ± 3	Q1041	Not Assigned
G931	-	T968	80 ± 30	A1005	41	A1042	-
L932	64 ± 5	V969	-	Q1006	-	R1043	-
V933	Not Assigned	D970	50 ± 20	Q1007	19 ± 2	L1044	-
K934	12.4 ± 0.9	E971	-	Y1008	-	K1045	-
A935	15 ± 1	S972	-	V1009	-	M1046	0.62 ± 0.06
V936	8 ± 3	L973	30 ± 10	M1010	-	I1047	-
I937	4 ± 3	P974	N/A	T1011	-	S1048	CLEANEX
E938	Not Assigned	V975	-	S1012	Not Assigned	Q1049	CLEANEX
M939	Not Assigned	L976	-	L1013	-	S1050	CLEANEX
S940	-	P977	N/A	Q1014	-	R1051	CLEANEX
S941	-	A978	-	Q1015	53	P1052	N/A
K942	-	S979	Not Assigned	E1016	-	H1053	CLEANEX
I943	-	T980	-	Y1017	-		
Q944	Not Assigned	H981	-	K1018	-		

Supplemental Table S1 Legend.

Hydrogen exchanges rates for the backbone amide protons of the FAT domain were measured by fast heteronuclear single quantum coherence (fHSQC) as a function of time for amide protons with exchange rates less than 0.1 min^{-1} . The exchange rates for the amide protons measured by fHSQC are shown in Supplementary Table 1 in units of 10^{-3} min^{-1} . The exchange rates of amide protons that were observed using the CLEANEX-PM method were not quantified and are labeled CLEANEX in the table. Proline residues do not contain an amide proton and are labeled N/A in the above table. Amide protons that were not assigned in the HSQC spectrum are labeled “Not Assigned”. Amide protons that were assigned, but not observed in either the first time point of the real-time exchange or the CLEANEX-PM method are denoted with a dash.



Supplemental Figure S1. Chemical Denaturation of the FAT Domain of FAK

Using Guanidine Hydrochloride (GdnHCl)

The ellipticity at 222 nm for the FAT domain of FAK was measured as a function of increasing guanidine hydrochloride concentration. Measured points are shown as filled circles and a global fitting of the denaturation curve, using the method of Santoro and Bolen (Santoro and Bolen, 1988), is shown as a solid line.

Supplemental References

Bahar, I., Wallqvist, A., Covell, D.G., and Jernigan, R.L. (1998). Correlation between native-state hydrogen exchange and cooperative residue fluctuations from a simple model. *Biochemistry* 37, 1067-1075.

Clementi, C., Nymeyer, H., and Onuchic, J.N. (2000). Topological and energetic factors: what determines the structural details of the transition state ensemble and "en-route" intermediates for protein folding? An investigation for small globular proteins. *J. Mol. Biol.* 298, 937-953.

Dokholyan, N.V., Borreguero, J.M., Buldyrev, S.V., Ding, F., Stanley, H.E., and Shakhnovich, E.I. (2003). Identifying importance of amino acids for protein folding from crystal structures. *Methods Enzymol.* 374, 616-638.

Santoro, M.M., and Bolen, D.W. (1988). Unfolding free energy changes determined by the linear extrapolation method. 1. Unfolding of phenylmethanesulfonyl a-chymotrypsin using different denaturants. *Biochemistry* 27, 8063-8068.

Shakhnovich, E.I. (1997). Theoretical studies of protein-folding thermodynamics and kinetics. *Curr. Opin. Struct. Biol.* 7, 29-40.

Vendruscolo, M., Paci, E., Dobson, C.M., and Karplus, M. (2003). Rare fluctuations of native proteins sampled by equilibrium hydrogen exchange. *J. Am. Chem. Soc.* 125, 15686-15687.